OXFORD UNIVERSITY PRESS | Behavioral Ecology

Species cumulative impacts on mixed assemblages of Neotropical parrots

Journal:	*Behavioral Ecology*
Manuscript ID	BEHECO-2024-0323.R1
Manuscript Type:	Original article
Keywords:	social status, pioneers, sentinels, brain size, dominance, reciprocal altruism

TITLE: Species cumulative impacts to mixed assemblages of Neotropical parrots

AUTHORS: Kyle S. Van Houtan,[1†*] Jose-Ignacio Rojas-Moscoso,[2] Hope N. Van Houtan,[3] Oscar Gonzalez[4,5]

AFFILIATIONS: [1] Center for Conservation Biology, Department of Biology, Stanford University, Stanford, California 94305, USA; [2] Environmental Studies, University of California, Santa Cruz, California 95064 USA; [3] The King's Academy, West Palm Beach, Florida 33411 USA; [4] College of Arts and Sciences, Anderson University, South Carolina 29621 USA, [5] Grupo Aves del Perú. Lima, Perú.

* Send correspondence to: kyle.vanhoutan@gmail.com

[†] Present address: Nicholas School of the Environment, Duke University, Durham, NC 27708 USA.

ACKNOWLEDGEMENTS: P. Ehrlich, G. Daily, and W. Durham provided academic and project support. E. Nycander, K. Holle, M. Feldman, J. Doble, P. Vas Dias, and A. Marker provided logistical and administrative support. R. Tamaki, B. Saenz, M. Napravnik, C. Ocampo-Raeder, D. Fernando, D. Ramon, D. Sabino, P. Deza, E. Caviedes, M. Gonzales, A. Stronza, C. Sekercioglu, A. Launer, C. Galindo-Leal, J. Gilardi, B. Griscom, T. Gangolet, J. Larsen, D. Brightsmith, C. Munn, and many additional *tigres* and *caballeros* advised and facilitated field operations. A. Kratter, S. Brady, L. DeCicco, L. Salinas, J. Trimble, M. Hagemann, K. Epperly, L. Beckman, and J. Gerwin provided access to museum specimens. N. Black and A. Files provided morphometric data, and S. Claramunt advised on bird wing ecomorphology. E. Hummel provided parrot images. S. Becker, T. Nicholson, and T. Gágne advised on the random forest model code and implementation. T. Clutton-Brock, G. Daily, S. Pimm, and anonymous reviewers improved earlier versions of this manuscript. KV thanks the physicians and staff of the Infectious Diseases Clinic at the Stanford Medical Center and K. Keilhacker, P. Davis, S. Scruggs, M. Yelton, S. Malladi, and C. Lobas who provided support.

AUTHOR CONTRIBUTIONS: KV designed the study, raised research support, administered the project, contributed data, entered and analyzed the data, wrote the code, performed the analysis, created the figures, and wrote the manuscript. JR, HV and OG contributed data and reviewed the manuscript.

DATA AVAILABILITY: All datasets and code used here are available at a third-party repository (GitHub, bit.ly/3qW45Md). *This repo is currently private and will become public when the manuscript is accepted for publication*.

COMPETING INTERESTS: All other authors declare no competing interests.

FUNDING: This research was supported by grants from the Morrison Institute for Population and Resource Studies, Center for Conservation Biology, and Anthropology Department at Stanford University. Rainforest Expeditions provided in-kind logistical support. Patagonia Inc. and The North Face Apparel Corp. provided material support for field expeditions.

TITLE: Species cumulative impacts on mixed assemblages of Neotropical parrots

RUNNING HEAD: mixed parrot groups

KEY WORDS: social status, pioneers, sentinels, brain size, dominance, reciprocal altruism

ABSTRACT 191 words

Mixed-species aggregations at fixed resources often demonstrate complex social structure and behaviors. However, these systems are underappreciated in behavioral ecology, ultimately limiting our understanding of population and community processes. Here we observed 13 species of parrots, macaws, and parakeets in foraging assemblages at exposed cliffs in southeast Perú. For each species, we developed a multivariate index of group impact by accumulating 9 separate metrics of abundance, chronology, functions, and interactions. This index appreciates species that join aggregations in large numbers, participate early, serve in functional roles, interact with others, and are socially dominant. We used Random Forest ("RF") algorithms to build nonlinear multiple regressions to assess and rank the influence of a suite of taxonomic and morphometric factors on this index. The RF models (R^2 = 0.96) indicate parrots with smaller brains (controlled for body size) have the highest impact scores, with several potential underlying mechanisms. We further document a distinct sequence of group participation where subordinate species serve as pioneers that initiate group assembly and foraging, while dominant species serve as sentinels, foraging after subordinates. This result suggests that sequenced tradeoffs and reciprocal altruism may be important in these mixed-species groups.

LAY SUMMARY 65 words

Birds demonstrate complex forms of social organization, especially in mixed-species groups. In Amazonian parrots, we show subordinate species were key for assembling groups and initiating foraging, while dominant species served as sentinels and foraged later. We developed an index that accumulated various species impacts to group aggregations and used machine learning to reveal that small brained and dispersal limited species had the most group impact.

INTRODUCTION 502 words

Animal social groups take many forms across taxa and ecosystems, playing key roles in shaping ecological communities (Doody et al., 2013; Ehrlich and Ehrlich, 1973; Holldobler and Wilson, 2009; Van Schaik, 1983). Group associations are widespread because they offer clear advantages: improved foraging success, reduced risk of predation, and fitness through kin selection (Krebs and Davies, 1993). Most animal societies are therefore monospecific, shaped by shared evolutionary histories, morphologies, and behaviors. However, structured mixed-species groups are also common (Goodale et al., 2017), especially among birds (e.g., Barnard and Thompson, 1985; Chapman et al., 1989; Darling, 1938; Morse, 1970), and are particularly prevalent in tropical forests (e.g., Hart and Freed, 2003; Munn and Terborgh, 1979; Thiollay, 1999).

Mixed-species bird flocks are typically classified by their dominant food resource or physical niche. Flocks that forage cooperatively within a stable home range, for instance, are labeled "mixed-species flocks" (*sensu stricto*), in contrast to those that track army ant swarms (*Eciton burchellii*) or congregate at localized resources like fruiting trees (Daily and Ehrlich, 1994;

Mangini et al., 2023; Powell, 1985; Terborgh et al., 1990). Forest strata further differentiate flock types. Understory flocks differ in microhabitat and species composition from canopy flocks, even though both may be territorial and organized around nuclear, sentinel, and leading species (Munn and Terborgh, 1979). Indeed, these social structures often coexist within the same forest, operating independently (Terborgh et al., 1990). Such niche-based classifications, however, may obscure the emergent properties and broader ecological roles of these assemblages (Carlson et al., 2023).

Compared to other forest birds, mixed groups of parrots (e.g., Chapman et al., 1989; Gilardi and Munn, 1998) are poorly understood, presenting an opportunity to describe their social dynamics. Conveniently, parrot flocks are often conspicuous and frequently aggregate at geographically fixed food resources, making them relatively easy to observe. In Perú, for example, large numbers of parrots, macaws, and parakeets gather daily at exposed cliff banks to forage on clay. Here, prior studies have documented their composition, seasonal patterns, and the physiological motivations for geophagy (Brightsmith and Muñoz-Najar, 2004; Brightsmith and Villalobos, 2011; Gilardi et al., 1999; Gilardi and Munn, 1998). Yet key aspects of their collective behavior remain largely unexplored. These include their abundance, communication, synchronization, hierarchy, and functional roles (e.g., Carlson et al., 2023; Clutton-Brock et al., 1999; Farine, 2022; Raihani, 2021; Trivers, 1971).

Through a collaboration among an indigenous community, an ecotourism enterprise, and a university (Brightsmith et al., 2008; Stronza and Durham, 2008), we monitored mixed-species parrot groups along the Tambopata river in southeastern Perú. We characterized flock composition, and documented cooperative behaviors, species roles, and antagonistic interactions. We refined existing quantitative methods by developing a multivariate index that summarizes social behavior, and we applied machine learning to assess how this index relates to a suite of taxonomic and morphometric traits. As a result, this study advances our understanding of parrot sociality, generates new methods for quantifying group impact, identifies potential underlying drivers of social behavior, and offers new insight into cooperation and altruism in mixed-species assemblages.

METHODS 1774 words

Field Site & Observations

The Tambopata Research Center ("TRC", -13.136358°, -69.609541°) is in the Tambopata province of the department of Madre de Dios in southeast Perú. Moist tropical broadleaf lowland forests consisting of terra firme, várzea, and bamboo characterize the region (Erwin, 1984; Foster et al., 1994). TRC lies within the 2,800 km^2 Tambopata National Reserve (IUCN category VI), immediately adjacent the Tambopata River and the 11,000 km^2 Bahuaja-Sonene National Park (IUCN category II). These protected areas have various access and resource extraction controls (Asner and Tupayachi, 2017; Kirkby et al., 2010). Along the Tambopata river, 750 m south of TRC, the study site is a 10m tall × 100m wide cliff of exposed clay. Locally it is known as the "collpa" (variously spelled as colpa or ccollpa).

During the dry season June–October 1999, we observed parrot activity (INRENA permit no. 53-99-9-INRENA-DGANPFS-DANP) in a camouflaged observation blind ~25m from the collpa base (Fig. 1). All counts and behavioral observations used binoculars (8×32, Leica, Trinovid BA), spotting scopes (15-40× zoom eyepiece, Bushnell, Spacemaster) and video cameras (Hi8 with 10× zoom, Sony, CCD-v801). At 30 minutes before morning twilight (defined as "civil dawn", data from: https://www.timeanddate.com/), we recorded the first audible parrot calls while hiking to the

observation blind. At this time, up to 16 species of Psittacidae parrots gather in the forest canopy above the collpa. From the blind, we recorded the time and composition of the first pioneer group that ritualistically flies above the collpa (locally called the "dance" cohort) searching for a place to land and forage. When this group landed, the dawn assemblage began.

At 5-minute intervals, an observer counted individual birds of each species on the collpa, until the dawn group ended (defined as when < 2 species remained). In addition to counts, a separate observer continuously recorded flock disturbances, sentinel alarms, and agonistic interactions. While birds typically clustered in single species groups (e.g., Fig. 1b-d), species also interacted, sometimes agonistically. When one bird displaced another on the collpa (through gape lunges, bites, wing beats, body pushing (Marcuk et al., 2020; Serpell, 1982), or by dropping debris) we recorded the winning and losing species. We also recorded flushes, defined as when > 50% of foraging or perched birds abruptly dispersed. When possible, we noted the cause (an obvious visual or audio cue) that immediately preceded the flush in the area where it occurred. For flushes preceded by alarm calls, we recorded the sentinel species making the alarm call (Fig. 1e).

We reviewed 40 hours of video to both confirm these observations and obtain additional data. While the dawn collpa activity required 2 observers, ≥ 1 remained until 16:00, recording the irregular collpa activity that occurred throughout the day. This monitoring protocol preceded and was only partially followed by subsequent studies (Brightsmith and Muñoz-Najar, 2004; Brightsmith and Villalobos, 2011).

Summarizing Group Activity

Following ecological footprint studies (Halpern et al., 2015; Halpern et al., 2012; Van Houtan et al., 2010), we synthesized observed bird activity using a multivariate index that accumulates each species' impact on group aggregations. We used the formula:

$$M = \sum_{j=1}^{n} \sum_{i=1}^{n} p_i n^{-1}$$

[Eqn. 1]

Where *i* represents 9 derived metrics, grouped into *j* categories—abundance, chronological sequence, functional roles, and interspecific interactions (see Table 1). This approach builds on previous indices of flocking propensity in birds that were based solely on presence/absence records (e.g., Jullien and Thiollay, 1998; Van Houtan et al., 2006), and incorporates metrics explicitly recommended in a recent review of mixed-species aggregations (Carlson et al., 2023). The resulting index, *M*, combines a fuller suite of separate participation and behavioral data that together capture the cumulative footprint of each species on the group dynamics.

Here, p_i is the quantity of each individual metric, rescaled from 0-100, where n^{-1} ensures equal weighting among categories. As a result, the maximum sum for each *j* category (i.e., the inner summation loop) is 100, and the maximum *M* index value for each species is 400 (i.e., the outer summation loop). As we are interested in the dynamics of mixed-species groups, all indices are calculated from observations of > 1 species. Additionally, due to the correlation between dawn and flock formation (e.g., Fig. 2, $R^2 = 0.77$, $p < 0.0001$) we rescaled all observation times to the elapsed time since civil dawn. Otherwise, observations from unadjusted time reports seasonal artifacts.

To account for group composition, we described species abundance both by individuals and by aggregate biomass. For individuals, we assumed counted birds remained for the duration of each 5-minute survey interval and convert this to an hourly rate. We summed the individuals in each discrete 5-minute window for all days and divide the total observation days. Given the broad range in bird sizes (0.07-1.2 kg), we separately multiplied the previous metric by species body mass (Brightsmith and Villalobos, 2011). To account for the sequence of species participation and how that influences group formation and maintenance, we calculated chronology across the full day and then within the dawn aggregations. The full-day chronology is the time of the peak biomass abundance for each species across all monitored daytime hours. Constrained to 0-2 hours after dawn, the morning flock chronology is the maximum value of a locally weighted regression (Cleveland and Devlin, 1988) fit to the abundance data against time.

To quantify functional roles for each species to the groups, we derived two metrics. The first tabulated the raw occurrences across the study period when each species participated in the dawn pioneer cohort. The second counted the times each species was an alarming sentinel. Due to the complexity of interspecific interactions, we developed 3 metrics to describe them. To account for social status, displacement rate was the number of wins divided by the total agonistic interactions observed for each species. Species interaction rate was the number of agonistic interactions divided by its individual abundance. Interaction breadth was the total number of species for which each species had agonistic interactions. Across measurement scales—metric, category, index)—*M* represents a single cumulative footprint derived from independent, relevant factors for these mixed-species groups.

	category		metric	description
a.	abundance	1	biomass	aggregate bird biomass (kg hr^{-1} day^{-1}) corrected for observer effort
	abundance	2	individuals	aggregate number of individual birds (birds hr^{-1} day^{-1}) corrected for observer effort
b.	chronology	3	full day	daily hour of maximum abundance, rescaled to hours after dawn
	chronology	4	dawn flock	time of peak value of a LOESS regression fit of dawn flock abundance against time
c.	functional roles	5	pioneer	occurrences when each species participated in the pioneer dawn cohort
	functional roles	6	sentinel	occurrences each species gave a sentinel alarm call, flushing the group
d.	interactions	7	displacement rate	number of times a species displaced another divided by the total agonistic interactions for that species
	interactions	8	interaction rate	total number of agonistic interactions with other species divided by the species' total daily individual abundance (metric 2)
	interactions	9	interaction breadth	the number of species with which each species had agonistic interactions

Table 1. Metrics composing the group impact index. Flock monitoring revealed 9 metrics of abundance, chronological sequence, functional roles, and agonistic interactions that impacted group formation, anti-predator vigilance, and social status. See Methods and Figs. 2-5 for more details.

We used non-parametric bootstrapping to generate a series for *M* with the above formula. For each species, we calculated Eq. [1] by randomly sampling the full set of *i* metrics *n*×*n* times (9 recursive samples for each 9 metrics) with replacement. We divide the result by *n* and replicate the process 2000 times. Each individual replicate is the average of Eq. [1] when repeated *n* times,

where each calculation of *M* is performed on a random sample (with replacement) of the complete set of 9 independent metrics. The resulting series is a statistically robust and cumulative accounting of species' impact to the group, where the weighting of each metric is randomized through resampling.

Species Level Covariates

We assembled a suite of potential model covariates from external morphometrics, flight aerodynamics, cognitive, and taxonomic features.

The ornithology collections of 8 institutions provided access to parrot specimens. These included the Carnegie Museum of Natural History, Museum of Comparative Zoology (Harvard University), University of Kansas Biodiversity Institute, Universidad Nacional Mayor de San Marcos (Perú), Florida Museum of Natural History (University of Florida), Burke Museum of Natural History and Culture, Bernice Pauahi Bishop Museum, and the Museum of Vertebrate Zoology (University of California). From study skins and spread wings, wing rules measured the wing chord (closed wing length, L_w) and the span from the carpal joint to the first secondary feather's tip (S_1) of each wing. Digital calipers recorded the straight culmen and lower mandible lengths. Body mass (Brightsmith and Villalobos, 2011) and brain volume (Schuck-Paim et al., 2008) are from published studies. Lacking the brain volume of *Brotogeris cyanoptera*, we averaged the values of 6 congeners. To visualize their forms, we imaged the spread wings and bills of focal species or their congeners on standardized grids. Schodde et al. (2013) gave tribe, genus, and species classifications.

We used the wing and bill measurements to calculate relevant metrics. The hand-wing index ("HWI") is correlated with dispersal ability (Claramunt et al., 2012; Claramunt and Wright, 2017) which is an important trait in Amazonian forest birds (Van Houtan et al., 2007). HWI equals $100*((L_w-S_1)/L_w)$. Total wing area is a key aerodynamic metric (Gagné et al., 2018b; Pennycuick, 2008), summarized by an index ("TWAI") that equals $3S_1L_w$ (Claramunt and Wright, 2017). Wing load is standard gravity × body mass × $TWAI^{-1}$ (Pennycuick, 2008). Bill lengths are correlated with social dominance (Daily and Ehrlich, 1994; Marcuk et al., 2020; Serpell, 1982) and we summed both measurements. To describe cognitive aptitude we corrected brain volume for body size (Mace et al., 1981), taking the residuals from best fit power model of the two series (Krebs and Davies, 1993).

Model Features and Computing libraries

In line with previous ecological studies (Becker et al., 2019; Becker et al., 2020; Gagné et al., 2018a; Gagné et al., 2018b; Nicholson et al., 2023; Nicholson et al., 2024), we used Random Forest ("RF") algorithms to build nonlinear multiple regressions to predict *M*. RF models are a machine learning tool with several advantages to linear least squares regression. RF models (i) are scalable to large datasets that include categorical and continuous data, (ii) accommodate both nonlinearity and heteroscedasticity, (iii) present ensemble conclusions of decision trees made from randomized subsets of predictor and response data, and (iv) facilitate visualizations of multiple predictors on the model outcomes (Breiman, 2001).

We trained an RF through resampling the dataset with 10-fold cross validation, set the number of model trees (*ntree* = 2000) and by tuning the number of available parameters at node splitting (*mtry*) for optimal performance. *K*-fold cross validation evaluated the model by splitting the data into *k* equally-sized sets; fitting it on the *k*-1 sets and testing it on the remaining hold-out

(Gareth et al., 2013). This routine looped for each *k* set, then summarized model performance by calculating the ensemble average R^2 across all *k* tests (we repeated the entire process 5 times). We initially tuned and ran an RF using all available covariates (n = 10), but as many variables were correlated, we retuned and ran an RF using only 5 inputs without performance loss. These inputs are tribe, brain size, cumulative bill straight length, HWI, and wing load.

The R statistical language (RCoreTeam, 2022) performed all analyses in macOS Sequoia 15.4.1 run on an 8-core M1 chip. The 'dplyr' and 'tidyr' libraries facilitated data wrangling and sampling (Wickham et al., 2023). The 'caret' and 'randomForest' libraries (Kuhn et al., 2020; Liaw and Wiener, 2002) trained, tuned, and fit RF regressions. The 'doParallel' library reduced computation times (Weston and Calaway, 2022). The 'pdp' library generated partial dependence data (Greenwell, 2017). A third-party repository (GitHub, bit.ly/3qW45Md) contains data and code.

RESULTS 1022 words

We documented 16 species of Neotropical parrots (subfamily Arinae) on the TRC collpa: 6 macaws, 5 parrots, 3 parakeets, and 2 parrotlets. The macaws included the red-and-green (*Ara chloroptera*, "RGMA"), blue-and-yellow (*Ara ararauna*, "BYMA"), scarlet (*Ara macao*, "SCMA"), chestnut-fronted (*Ara severus*, "CFMA"), and red-bellied (*Orthopsittaca manilatus*, "RBMA"). The parrots are the mealy amazon (*Amazona farinosa*, "MEPA"), yellow-crowned amazon (*Amazona ochrocephala*, "YCPA"), blue-headed (*Pionus menstruus*, "BHPA"), white-bellied (*Pionites leucogaster*, "WBPA"), and orange-cheeked (*Pyrilia barrabandi*, "OCPA"). The parakeets are the white-eyed (*Psittacara leucophthalmus*, "WEPA"), dusky-headed (*Aratinga weddellii*, "DHPA"), and cobalt-winged (*B. cyanoptera*, "CWPA"). We observed dusky-billed (*Forpus modestus*) and Amazonian (*Nannopsiottaca dacchileae*) parrotlets at the collpa but only in monospecific flocks after dawn. One additional macaw—blue headed (*Primolius couloni*)—was more furtive and occasionally seen perched in the trees above the feeding flocks. We consider neither *F. modestus*, *N. dacchileae*, nor *P. couloni* further. With the available technology (see Methods), the small macaws—RBMA and CFMA—evaded distinction while foraging and we lumped their observations as "GRMA." We further analyze 11 species and 1 species complex (GRMA).

Above and on the collpa, we observed various groupings and activities (Fig. 1). The most pronounced activity occurred in aggregations immediately after dawn (Fig. 1b). Smaller—predominantly single species (Fig. 1c-d)—groups occurred sporadically throughout the day. All species foraging on the collpa also perched in the vegetation above it (Fig. 1e), where some would sound alarms (Fig. 1f). Though up to 9 nine species and nearly 350 birds could be seen foraging on the collpa at one time, dawn flocks typically attained a maximum richness of 6 species, peak abundance of 200 birds and peak activity 10-20 min. after flocks initially formed (Fig 1g-h). Dawn flocks followed a consistent sequence of events and behavior: sunrise, audible calls, pioneer cohort dance, pioneer cohort lands, birds continuously arriving and leaving the foraging group, and the group ending (Fig. 2). Though dawn flocks might last > 80 min., the median duration was 53 min. (Fig. 2b). The dance cohort was typically brief (median = 3 min.) and was tightly fixed to the timing of dawn (Fig. d-e). Over 99 days, researchers observed 583 daylight hours biased toward dawn, with a cumulative 749 observer hours spread over 79 discrete days (Fig. 2f-g).

Species demonstrated distinct chronologies of activity, with most (8 of 12) preferring dawn flocks (Fig. 3a). Assessed by total and peak abundance (Fig. 3a-b), 2 species (BYMA, SCMA) regularly joined both dawn and day groups, while 2 others preferred day groupings (RGMA, CWPA). Whether ranked by biomass or individuals, BHPA and MEPA are the most abundant species

recorded (Fig. 3c-d). We observed 50 BHPA and 30 MEPA individual birds hr^{-1} in each dawn group. Most species (n = 8), however, have ≤ 5 birds hr^{-1} in the dawn flocks. Within the dawn groups, species also demonstrated distinct chronology preferences (Fig. 4). Though congeners, YCPA is the first species to arrive, and MEPA is second to last (Fig. 4a-b). The 3 earliest arriving species comprise the only pioneers who lead dance sorties (Fig. 4c). This included both small macaws (CFMA, RBMA) that while easily differentiated in flight, were not distinguished by their dorsal plumage while foraging.

Flushes were common in dawn groups (mean = 15.5 day^{-1}), though most (999/1200, 83.3%) were not attributed to a direct cause (Fig. 5a). For flushes that were, 163 (13.6%) were anthropogenic and 38 (3.2%) natural causes. The leading known cause was tourist boats and tourists viewing parrots from conspicuous trails above the collpa (Fig. 5b). The leading known natural flush cause was birds of prey (*Falco deiroleucus* and *Astur bicolor* attempted depredations of OCPA, WEPA, and DHPA). Flushes preceded by sentinel alarms (n = 187) were unevenly distributed across 10 species (Fig. 5c). Four of the most common sentinels were late foragers in dawn groups (Fig. 4a). Interspecific interactions revealed their prevalence and hierarchical status (Fig. 5d-e). BYMA, YCPA, and GRMA frequently interacted with many species, while SCMA, CWPA, and RGMA frequently interacted with few species (Fig. 5d). Status largely reflects body size (Fig. 5e). The largest species, RGMA, was uniquely dominant, winning > 50% of all interactions. The smallest species, CWPA, was always subordinate with 0 wins.

The cumulative impact index, M, reflects individual metrics of abundance (Figs. 3), chronology (Figs 3-4), functional roles (Figs. 4-5), and interactions (Fig. 5). This cumulative footprint appreciates species (e.g., BHPA, MEPA) that have high abundance, participate early in dawn flocks, perform group-serving functions, and interact frequently with many other species while winning most interspecific interactions. Conversely, M relegates species (CWPA, WBPA) that do not express these traits. A non-parametric bootstrap routine created 2000 M values for each species retaining the rankings of the raw scores from Eqn [1] while randomly resampling them (Fig. 6a-b).

Museum specimens and published data reveal a range of morphometric indices relevant for status, flight, and cognition (Fig. 7). Large macaws have the largest bills (Fig. 7c), small macaws and parakeets have the greatest dispersal ability (Fig. 7d), and the amazons have the highest wing loads (Fig. 7e). The fitted power model of brain size to body mass has an exponent of 0.70 [remarkably consistent with fitted relationships in birds (Krebs and Davies, 1993)], revealing differences among congeners and species (Fig. 7f).

The morphometric and taxonomic variables display a variety of pair-wise relationships to M (Fig. 8). M increases as brain size (adjusted for body mass) decreases (Fig. 8a). Aerodynamic metrics have inconsistent relationships (Fig. 8b,e), bill size has a mid-domain peak (Fig. 8c) while the Androglossini tribe is above Arini (Fig. 8d). The trained, tuned, and optimized RF model performs well (R^2 = 0.959), ranking brain size ahead of HWI, bill length, wing load, and tribe (Fig. 8f). Model performance was insensitive both to removing correlated predictors and resampling procedures (see Methods). Partial dependence plots display bivariate influences on model predictions, y^ (Fig. 8g-j). The confluence of small brains, small HWIs, high wing loads and medium bills predict high sociality (Fig. 8g-h). Tribe has a negligible influence (Fig. 8j).

DISCUSSION 1342 words

Here we developed novel means to accumulate various traits of group aggregations and model their drivers with machine learning. Our main result is deriving a multivariate index, M, and

documenting its relationship to brain size. Fig. 8f shows that brain size is the strongest predictor of *M*, outperforming all factors. This suggests parrot species with smaller brains have the most impact on structuring groups, perhaps as they stand to gain the most from the aggregations. As observed in other animal social groups, such cooperation might increase foraging opportunities, foraging efficiency, and antipredator vigilance (Ehrlich and Ehrlich, 1973; Krebs and Davies, 1993; Moynihan, 1962; Powell, 1985; Terborgh, 1990)—presumably increasing benefits and reducing risks to survival and fitness (Krebs and Davies, 1993). An alternative explanation for this result derives from expensive tissue theory. As seen in mammals, frogs, and birds (Aiello and Wheeler, 1995; Isler and van Schaik, 2006; Liao et al., 2016), this suggests species with larger brains possess a comparative reduction in other metabolically demanding tissues, such as the gut. Small-brained parrots may therefore have higher *M* scores as they may be predisposed to benefit most from geophagy itself. Small-brained parrots may have correspondingly larger digestive tracts and are, therefore, most able to process clays and extract their nutrients. This is currently speculative; however, it merits further examination in this context and in mammal aggregations at mineral licks (Griffiths et al., 2020; Griffiths et al., 2023).

The combination of observed pioneer, sentinel, and status data suggest reciprocal altruism functions between species. Foraging on the exposed collpa poses measurable risk, as birds perch conspicuously in open areas with their vision often restricted in cliff recesses (Fig. 1a,f). Bird assemblages as a result are hyper-vigilant, frequently alarming and flushing to safety (Fig. 5a). Here an interesting tradeoff and separation of roles emerges. The 3 most vigilant sentinels (Fig. 5c: MEPA, SCMA, BYMA) are the most antagonistic, dominant (Fig. 5d-e), and among the later species in the dawn flock sequence (Fig. 4a-b). Pioneer species seldom serve as sentinels and the commonest sentinels are never in the leading dance cohort (Fig. 4c). As a result, sentinel species guard before feeding, sounding alarms from perches in vegetation above the collpa. When it is their turn to feed, sentinels land on the collpa where they often displace the feeding positions of pioneer species who previously established foraging perches. Sentinels continue to sound alarms from the collpa and from perches above it. Though most single-species social groups have pioneer and sentinel roles (Clutton-Brock et al., 1999), here the roles are split between species. Other mixed-species groups also split such roles between species, but in those groups the roles occur while all species forage simultaneously (Hart and Freed, 2003; Moynihan, 1962; Munn and Terborgh, 1979; Powell, 1985; Terborgh et al., 1990; Van Houtan et al., 2006). In these parrot assemblages, the roles appear characteristically sequenced in time. Dominant, highly interactive sentinels like MEPA might delay foraging by > 20 min. or more after subordinate pioneers like BHPA.

Congeners that shared many morphological traits also had distinct behaviors. The only Amazon parrots, MEPA and YCPA, have highly similar body, bill, wing, and brain metrics (Fig. 7). Ultimately, these are the top 2 ranked species in the sociality index, but they arrive there via different means (Fig. 6). YCPA is a core species in the pioneer cohorts where MEPA is a late arriving species in the dawn flock and the most common sentinel (Fig. 4, 5c). Our observations suggest their participation in foraging assemblages is almost mutually exclusive. Furthermore, the 3 large *Ara* macaws also have similar morphometrics (Fig. 7), are key sentinels (Fig. 5c) and are dominant over other species (Fig. 5e). However, RGMA rarely join dawn flocks, where BYMA and SCMA prefer them (Fig. 3a). Interestingly, BYMA has a noticeably smaller brain than either RGMA or SCMA which may motivate its higher *M* score (Fig. 6, 7f). Differences in the social behaviors among closely related congeners in such mixed-species groups deserve more attention.

Future inquiries will improve on the present analysis. In all respects, ultra-high-definition digital imagery and video will advance the efficiency, ability, and precision of monitoring. This will

help identify cryptic (e.g., GRMA) and uncommon (*N. dacchileae*, *P. couloni*) species, resolve the attribution of flock threats and sentinel alarms (Fig. 5bc), reveal additional fine-scale interactions between species (Fig. 5d-e), and describe additional behaviors and hierarchies within species (Camerlenghi et al., 2022; Papageorgiou et al., 2019). Improved monitoring technology may also document the patterns, syntax, and significance of parrot vocalizations in such gatherings. New estimations of total bird wing area (Fu, 2022) may further characterize flight performance, but require wingspans which are not measured from folded-wing study skins. Capture, marking, and biotelemetry would yield unprecedented insights into individual movement and habitat use, but present significant logistical challenges. [Photographic identification of individuals is a potential non-invasive, alternative technique (Núñez-López et al., 2021).] In combination with biotelemetry and monitoring, feather 'omics using either bulk or compound-specific stable isotope analysis (Gagné et al., 2018b; Van Houtan et al., 2024) would provide important diagnostic data on diet and trophic status. Lastly, as they tend to range widely and more frequently encounter human hazards (Laurance et al., 2011; Van Houtan et al., 2007; Woodroffe and Ginsberg, 1998), obligate social species may become more prone to local extinction. Future attention to the relationship between cumulative indices of social impact (like *M*) and population status in social parrots, especially outside of protected areas, is important.

As unsupervised statistical procedures have the potential of spurious correlations and overfitting (Gareth et al., 2013), our final model reduced the number of variables, averaged results from a large number of trees, and deployed cross-validation. The resulting RF avoids bias and is curated to the smallest set of taxonomic and morphometric predictors with directly relevant mechanisms. Bill size was the only unadjusted variable for body size as it is a leading predictor of parrot aggression (Marcuk et al., 2020; Serpell, 1982). We optimized model performance by tuning the *mtry* hyperparameter from a possible range of values of 1:5. Factor rankings were insensitive to this tuning, but larger *mtry* values skewed how factors ranked. Though our analysis is a trait-based approach (Debastiani et al., 2021), it is constrained within the subfamily Arinae. Within this taxon, it remains possible that the data are phylogenetically structured (Felsenstein, 1985). While this does not violate decision-tree-based model assumptions [as it does for linear least squares regressions (Bielby et al., 2010)], we took several measures to identify potential artifacts. First, out of 10 predictors, species and genus were the 2 poorest performing predictors in our initial RF model (14% and 2% relative ΔMSE, respectively). Second, in our final RF, the only remaining taxonomic variable again performed poorest (tribe: 3% relative ΔMSE, Fig. 8f). Third, most of the remaining predictors (brain size, HWI, wing load) in the final model were corrected for the broad taxonomic influence of body size. Finally, we ran 2 *post hoc* RFs with the data split by tribe. In each single-tribe RF, brain size was ranked highly (Arini: 100% relative ΔMSE, Androglossini: 94% relative ΔMSE).

This study provides a comprehensive framework for describing the abundance and behavior of species in mixed assemblages, and provides further evidence that birds are a compelling taxon for studying animal collectives (Farine, 2022; Gonzalez, 2019). We observed distinct patterns of the abundance and chronology of flock participation for 13 parrot species (Figs. 1-4). Beyond basic membership, species displayed canonical functions as pioneer and sentinel species (Figs. 4-5). Agonistic interactions (Fig. 5) revealed a dominance hierarchy, with several pioneer species being subordinate and sentinels being dominant: partitioning and delaying the predictably sequenced foraging of sentinels. Our multivariate index of sociality derived from these data was best explained by brain size (Figs. 6-8), providing a basis for future studies to examine further the physiological benefits of geophagy and the potential roles of cognition, gut processing, flight performance, or other species traits, as well as any broader relationship between relative brain size and social behavior in mixed-species groups.

OPEN ACCESS, DATA AVAILABILITY STATEMENT: All datasets and code used here are available at a third-party repository (bit.ly/3qW45Md).

COMPETING INTERESTS: All other authors declare no competing interests.

REFERENCES

Aiello LC, Wheeler P, 1995. The expensive-tissue hypothesis: the brain and the digestive system in human and primate evolution. Current Anthropology 36:199-221.

Asner GP, Tupayachi R, 2017. Accelerated losses of protected forests from gold mining in the Peruvian Amazon. Environmental Research Letters 12:094004.

Barnard CJ, Thompson DB, 1985. Gulls and plovers: the ecology and behavior of mixed-species feeding groups. London UK: Croom Helm.

Becker SL, Brainard RE, Van Houtan KS, 2019. Densities and drivers of sea turtle populations across Pacific coral reef ecosystems. PLoS ONE 14:e0214972. doi: 10.1371/journal.pone.0214972.

Becker SL, Nicholson TE, Mayer KA, Murray MJ, Van Houtan KS, 2020. Environmental factors may drive the post-release movements of surrogate-reared sea otters. Frontiers in Marine Science 7:539904.

Bielby J, Cardillo M, Cooper N, Purvis A, 2010. Modelling extinction risk in multispecies data sets: phylogenetically independent contrasts versus decision trees. Biodiversity and Conservation 19:113-127.

Breiman L, 2001. Random forests. Machine learning 45:5-32.

Brightsmith DJ, Muñoz-Najar RA, 2004. Avian Geophagy and Soil Characteristics in Southeastern Peru. Biotropica 36:534-543.

Brightsmith DJ, Stronza A, Holle K, 2008. Ecotourism, conservation biology, and volunteer tourism: A mutually beneficial triumvirate. Biological conservation 141:2832-2842.

Brightsmith DJ, Villalobos EM, 2011. Parrot behavior at a Peruvian clay lick. The Wilson Journal of Ornithology 123:595-602.

Camerlenghi E, McQueen A, Delhey K, Cook CN, Kingma SA, Farine DR, Peters A, 2022. Cooperative breeding and the emergence of multilevel societies in birds. Ecology Letters 25:766-777. doi: https://doi.org/10.1111/ele.13950.

Carlson NV, Freeberg TM, Goodale E, Theo AH, 2023. Mixed-species groups and aggregations: shaping ecological and behavioural patterns and processes. Philosophical Transactions of the Royal Society B: Biological Sciences 378:20220093. doi: doi:10.1098/rstb.2022.0093.

Chapman C, Chapman L, Lefebvre L, 1989. Variability in parrot flock size: possible functions of communal roosts. The Condor 91:842-847.

Claramunt S, Derryberry EP, Remsen Jr J, Brumfield RT, 2012. High dispersal ability inhibits speciation in a continental radiation of passerine birds. Proceedings of the Royal Society B: Biological Sciences 279:1567-1574.

Claramunt S, Wright NA, 2017. Using museum specimens to study flight and dispersal. The extended specimen: emerging frontiers in collections-based ornithological research:127-141.

Cleveland WS, Devlin SJ, 1988. Locally weighted regression: an approach to regression analysis by local fitting. Journal of the American statistical association 83:596-610.

Clutton-Brock TH, O'Riain MJ, Brotherton PNM, Gaynor D, Kansky R, Griffin AS, Manser M, 1999. Selfish Sentinels in Cooperative Mammals. Science 284:1640-1644. doi: doi:10.1126/science.284.5420.1640.

Daily GC, Ehrlich PR, 1994. Influence of social status on individual foraging and community structure in a bird guild. Oecologia 100:153-165.

Darling FF, 1938. Bird flocks and the breeding cycle; a contribution to the study of avian sociality. Cambridge UK: Cambridge University Press.

Debastiani VJ, Bastazini VA, Pillar VD, 2021. Using phylogenetic information to impute missing functional trait values in ecological databases. Ecological Informatics 63:101315.

Doody JS, Burghardt GM, Dinets V, 2013. Breaking the social–non-social dichotomy: a role for reptiles in vertebrate social behavior research? Ethology 119:95-103.

Ehrlich PR, Ehrlich AH, 1973. Coevolution: heterotypic schooling in Caribbean reef fishes. The American Naturalist 107:157-160.

Erwin TL, 1984. Tambopata Reserved Zone, Madre de Dios, Peru: history and description of the reserve. Revista Peruana de Entolomogía 27:1-8.

Farine DR, 2022. Collective action in birds. Current Biology 32:R1140-R1144. doi: 10.1016/j.cub.2022.08.035.

Felsenstein J, 1985. Phylogenies and the comparative method. The American Naturalist 125:1-15.

Foster RB, Parker III T, Gentry AH, Emmons LH, Chicchon A, Schulenberg T, Rodriguez L, Lamas G, Ortega H, Icochea J, 1994. The Tambopata-Candamo reserved zone of southeastern Perú: a biological assessment. Washington, DC: Conservation International 184.

Fu HY, 2022. A New Method for Estimating Total Wing Area to Determine Flight Efficiency and Dispersal Ability in Birds: University of Toronto (Canada).
Gagné TO, Hyrenbach KD, Hagemann ME, Bass OL, Pimm SL, MacDonald M, Peck B, Van Houtan KS, 2018a. Seabird Trophic Position Across Three Ocean Regions Tracks Ecosystem Differences. Frontiers in Marine Science 5. doi: 10.3389/fmars.2018.00317.
Gagné TO, Hyrenbach KD, Hagemann ME, Van Houtan KS, 2018b. Trophic signatures of seabirds suggest shifts in oceanic ecosystems. Science Advances 4:eaao3946.
Gareth J, Daniela W, Trevor H, Robert T, 2013. An introduction to statistical learning: with applications in R: Spinger.
Gilardi JD, Duffey SS, Munn CA, Tell LA, 1999. Biochemical functions of geophagy in parrots: detoxification of dietary toxins and cytoprotective effects. Journal of Chemical Ecology 25:897-922.
Gilardi JD, Munn CA, 1998. Patterns of activity, flocking, and habitat use in parrots of the Peruvian Amazon. The Condor 100:641-653.
Gonzalez O, 2019. Trends in the Ecology and Evolution of Birds. Trends in Ecology & Evolution 34:879-880.
Goodale E, Beauchamp G, Ruxton GD, 2017. Mixed-species groups of animals: behavior, community structure, and conservation: Academic Press.
Greenwell BM, 2017. pdp: An R package for constructing partial dependence plots. The R Journal 9:421.
Griffiths BM, Bowler M, Gilmore MP, Luther D, 2020. Temporal patterns of visitation of birds and mammals at mineral licks in the Peruvian Amazon. Ecology and Evolution 10:14152-14164. doi: https://doi.org/10.1002/ece3.7006.
Griffiths BM, Jin Y, Griffiths LG, Gilmore MP, 2023. Physical, landscape, and chemical properties of Amazonian interior forest mineral licks. Environmental Geochemistry and Health 45:3263-3276. doi: 10.1007/s10653-022-01412-8.
Halpern BS, Frazier M, Potapenko J, Casey KS, Koenig K, Longo C, Lowndes JS, Rockwood RC, Selig ER, Selkoe KA, 2015. Spatial and temporal changes in cumulative human impacts on the world's ocean. Nature communications 6:7615.
Halpern BS, Longo C, Hardy D, McLeod KL, Samhouri JF, Katona SK, Kleisner K, Lester SE, O'Leary J, Ranelletti M, Rosenberg AA, Scarborough C, Selig ER, Best BD, Brumbaugh DR, Chapin FS, Crowder LB, Daly KL, Doney SC, Elfes C, Fogarty MJ, Gaines SD, Jacobsen KI, Karrer LB, Leslie HM, Neeley E, Pauly D, Polasky S, Ris B, St Martin K, Stone GS, Sumaila UR, Zeller D, 2012. An index to assess the health and benefits of the global ocean. Nature 488:615-620. doi: 10.1038/nature11397.
Hart PJ, Freed LA, 2003. Structure and dynamics of mixed-species flocks in a Hawaiian rain forest. The Auk 120:82-95.
Holldobler B, Wilson EO, 2009. The superorganism: the beauty elegance and strangeness of insect societies: WW Norton & Company.
Isler K, van Schaik C, 2006. Costs of encephalization: the energy trade-off hypothesis tested on birds. Journal of Human Evolution 51:228-243.
Jullien M, Thiollay JM, 1998. Multi-species territoriality and dynamic of neotropical forest understorey bird flocks. Journal of Animal Ecology 67:227-252.
Kirkby CA, Giudice-Granados R, Day B, Turner K, Velarde-Andrade LM, Dueñas-Dueñas A, Lara-Rivas JC, Yu DW, 2010. The market triumph of ecotourism: an economic investigation of the private and social benefits of competing land uses in the Peruvian Amazon. PloS one 5:e13015.
Krebs JR, Davies NB, 1993. An introduction to behavioural ecology. Oxford UK: Blackwell Scientific.
Kuhn M, Wing J, Weston S, Williams A, Keefer C, Engelhardt A, Cooper T, Mayer Z, Kenkel B, Team RC, 2020. Package 'caret'. The R Journal 223:48.
Laurance WF, Camargo JLC, Luizão RCC, Laurance SG, Pimm SL, Bruna EM, Stouffer PC, Williamson BG, Benítez-Malvido J, Vasconcelos HL, Van Houtan KS, Zartman CE, Boyle SA, Didham RK, Andrade A, Lovejoy TE, 2011. The fate of Amazonian forest fragments: A 32-year investigation. Biological Conservation 144:56-67. doi: DOI: 10.1016/j.biocon.2010.09.021.
Liao WB, Lou SL, Zeng Y, Kotrschal A, 2016. Large brains, small guts: the expensive tissue hypothesis supported within anurans. The American Naturalist 188:693-700.
Liaw A, Wiener M, 2002. Classification and regression by randomForest. R news 2:18-22.
Mace GM, Harvey PH, Clutton-Brock T, 1981. Brain size and ecology in small mammals. Journal of Zoology 193:333-354.
Mangini GG, Rutt CL, Sridhar H, Buitron G, Muñoz J, Robinson SK, Montaño-Centellas F, Zarco A, Fanjul ME, Fernández-Arellano G, Xing S, Camerlenghi E, 2023. A classification scheme for mixed-species bird flocks. Philos Trans R Soc Lond B Biol Sci 378:20220100. doi: 10.1098/rstb.2022.0100.
Marcuk V, Purchase C, de Boer D, Bürkle M, Scholtyssek K, 2020. Qualitative description of the submission and agonistic behavior of the Spix's Macaw (*Cyanopsitta spixii*, Spix 1824), with special reference to the displacement displays. Journal of Ethology 38:253-270.
Morse DH, 1970. Ecological aspects of some mixed-species foraging flocks of birds. Ecological monographs 40:119-168.
Moynihan MH, 1962. The organization and probable evolution of some mixed species flocks of neotropical birds. Smithsonian Miscellaneous Collection 1:1-140.
Munn CA, Terborgh JW, 1979. Multi-species territoriality in Neotropical foraging flocks. The Condor 81:338-347.

Nicholson TE, Mayer KA, Hazan SH, Murray MJ, Van Houtan KS, DeAngelo CM, Johnson AB, Fujii JA, 2023. Advancing surrogate-rearing methods to enhance southern sea otter recovery. Biological Conservation 281:109962. doi: 10.1016/j.biocon.2023.109962.
Nicholson TE, McClenachan L, Tanaka KR, Van Houtan KS, 2024. Sea otter recovery buffers century-scale declines in California kelp forests. PLOS Climate 3:e0000290. doi: 10.1371/journal.pclm.0000290.
Núñez-López B, Rivera-Ortíz FA, Soberanes-González CA, Arizmendi MdC, 2021. Differentiation of Military Macaws (Ara militaris) in captivity using photo-identification. Revista Mexicana de Biodiversidad 92.
Papageorgiou D, Christensen C, Gall GEC, Klarevas-Irby JA, Nyaguthii B, Couzin ID, Farine DR, 2019. The multilevel society of a small-brained bird. Current Biology 29:R1120-R1121. doi: https://doi.org/10.1016/j.cub.2019.09.072.
Pennycuick CJ, 2008. Modelling the flying bird. Cambridge, MA: Academic Press.
Powell GV, 1985. Sociobiology and adaptive significance of interspecific foraging flocks in the Neotropics. Ornithological Monographs:713-732.
Raihani N, 2021. The social instinct: how cooperation shaped the world. New York, NY: St. Martin's Press.
RCoreTeam, 2022. R: A language and environment for statistical computing (version 4.2.2). Vienna, Austria: R Foundation for Statistical Computing.
Schodde R, Remsen J, Schirtzinger EE, Joseph L, Wright TF, 2013. Higher classification of New World parrots (Psittaciformes; Arinae), with diagnoses of tribes. Zootaxa 3691:591-596.
Schuck-Paim C, Alonso WJ, Ottoni EB, 2008. Cognition in an ever-changing world: climatic variability is associated with brain size in neotropical parrots. Brain, Behavior and Evolution 71:200-215.
Serpell JA, 1982. Factors influencing fighting and threat in the parrot genus *Trichoglossus*. Animal Behaviour 30:1244-1251.
Stronza A, Durham WH, 2008. Ecotourism and conservation in the Americas. Oxfordshire, UK: CAB International
Terborgh J, 1990. Mixed flocks and polyspecific associations: costs and benefits of mixed groups to birds and monkeys. American Journal of Primatology 21:87-100.
Terborgh J, Robinson SK, Parker III TA, Munn CA, Pierpont N, 1990. Structure and organization of an Amazonian forest bird community. Ecological Monographs 60:213-238.
Thiollay J-M, 1999. Frequency of mixed species flocking in tropical forest birds and correlates of predation risk: an intertropical comparison. Journal of Avian Biology:282-294.
Trivers RL, 1971. The evolution of reciprocal altruism. The Quarterly review of biology 46:35-57.
Van Houtan KS, Gagné TO, Banko P, Hagemann ME, Peck RW, Yarnes CT, 2024. Climatic drought and trophic disruption in an endemic subalpine Hawaiian forest bird. Biological Conservation 299:110823. doi: https://doi.org/10.1016/j.biocon.2024.110823.
Van Houtan KS, Hargrove SK, Balazs GH, 2010. Land use, macroalgae, and a tumor-forming disease in marine turtles. PLoS One 5:e12900.
Van Houtan KS, Pimm SL, Bierregaard RO, Lovejoy TE, Stouffer PC, 2006. Local extinctions in flocking birds in Amazonian forest fragments. Evolutionary Ecology Research 8:129-148.
Van Houtan KS, Pimm SL, Halley JM, Bierregaard RO, Lovejoy TE, 2007. Dispersal of Amazonian birds in continuous and fragmented forest. Ecology Letters 10:219-229.
Van Schaik CP, 1983. Why are diurnal primates living in groups? Behaviour:120-144.
Weston S, Calaway R, 2022. Getting Started with doParallel and foreach. https://cranr-projectorg/web/packages/doParallel/vignettes/gettingstartedParallelpdf.
Wickham H, François R, Henry L, Müller K, Vaughan D, 2023. dplyr: A Grammar of Data Manipulation. R package version 114. doi: https://dplyr.tidyverse.org.
Woodroffe R, Ginsberg JR, 1998. Edge effects and the extinction of populations inside protected areas. Science 280:2126-2128.

Figure 1. Parrot assemblages feeding on clay cliffs in Tambopata, Perú. (a) A ~100m wide transect of exposed dirt revealing stratigraphic clay layers below *várzea* forest. Labelled cliff regions correspond to figure panels, with the Tambopata river and observer blind (denoted by *) in the foreground. (b) Mixed-species aggregation that gathers near dawn, here contains 6 species: mealy amazon (*A. farinosa*), blue-headed parrot (*P. menstruus*), orange-cheeked parrot (*P. barrabandi*), chestnut-fronted macaw (*A. severus*), blue-and-yellow macaw (*A. ararauna*), and scarlet macaw (*A. macao*). (c) Cobalt-winged parakeets (*B. cyanoptera*) and (d) red-and-green macaws (*A. chloroptera*) forage throughout the day, often in single species groups. (e) Mealy amazons perched in a nearby tree serving as sentinels, sounding alarm calls to warn other birds of threats. (f) Bill markings on exposed cliff surface reveal mineral-rich clays. (g-h) Raw data (circles) and summaries (boxplots) of abundance and species richness of birds foraging in dawn groups (n = 79). Thick line is a locally weighted regression, points are slightly jittered. Though foraging bouts may last over 80 minutes, peak abundance and richness occurs 10 and 20-25 minutes, respectively, after groups begin foraging. Images (c-e) provided by E. Hummel and used with permission. All other images from authors.

Figure 2. Dawn parrot assemblages have a characteristic behavioral sequence. (a) Raw observations (circles) and loess models (lines) document the sequence of dawn, first vocalization, multispecies pioneer cohort that circles the cliff face before landing ("dance"), first group landing, and the end of group foraging. Density plots show the median duration of (b) morning groups is 53 minutes and (c) dance flights is 3 minutes. The (d) median time elapsed from dawn to the dance is 35 minutes, and (e) a linear model of dawn hour to dance hour shows their correlation. Over a span of 99 days, observers monitored the clay cliff (f) from dawn until late afternoon, observing 583 daylight hours, with (g) 783 observer hours over 79 discrete days.

Figure 3. Observed species abundance of dawn and day mixed-species parrot groups. (a-b) Corrected for effort, species abundances map their chronology and peak occurrence. Uncommon in dawn groups, (b) cobalt-winged parakeets (CWPA) and red-and-green macaws (RGMA) preferentially forage ~ 7-9 hours after dawn. As the entire species set represents a range of sizes, we express total abundance in (c) biomass, and (d) number of individuals. Mealy amazon (MEPA) and blue-headed parrot (BHPA) top both lists. Panels in (a) are sorted chronologically by maximum species abundance, vertical grey lines border the 2 hours after dawn. Filled-circle color symbology retained in (b-d). Due to the technological difficulty of distinguishing small macaws on the cliff, "GRMA" combines red-bellied macaw (*O. manilatus*) and chestnut-fronted macaw (*A. severus*) observations. See Methods for all species codes.

Figure 4. Species sequence and pioneers in the dawn assemblages. When considering dawn groups alone, species show distinct early, middle, and late arrival patterns. For each species in (a), grey line is a loess model of abundance, whose (b) maximum value defines sequence differences. Though both are congeners and dawn-focused species, the yellow-crowned amazon is the first to arrive while the mealy amazon is last. (c) Observed pioneer species from dance cohorts are first to land and therefore establish the dawn assemblage. Both small macaw species are pioneers. Relative time is rescaled from the raw elapsed time from formation to end.

Figure 5. Flushes, sentinel alarms, and species interactions. (a) Groups abruptly flushing is common and has (b) various causes. All anthropogenic known causes are ecotourism related: boats ferrying guests to view the dawn flocks, exposed tourists on the trails above the cliff, and unconcealed tourists on the observation beaches facing the collpa below. Flush events are often preceded by alarm calls from sentinel birds perched in canopy trees. (c) Though 10 species served as sentinels, the most vigilant species (MEPA, SCMA) arrive late to forage in dawn flocks (Fig. 4ab). We observed 1,268 agonistic interactions between species, where an individual from one species

displaces the foraging perch of another. Grey lines in (d) are the median values of each axis, defining four quadrants of interactions: (I) frequent interactions with many species, (II) few with many species, (III) frequent with few species, and (IV) few with few species (see Methods). (e) Large-bodied macaws and amazons are dominant. Vertical grey line is the 50% displacement (win) rate, circle size is the number of interactions, error bar is standard error.

Figure 6. Multivariate index, *M*, derives and ranks species social impact. (a) Using Eqn. [1], *M* accumulates values from 9 distinct observations (each rescaled to 0-100) across four independent categories to synthesize a species impact on group assemblages. (b) Nonparametric bootstrapping generated a series of *M* values through random sampling with replacement (see Methods). This results in a statistically robust, cumulative footprint of derived from independent metrics of social impact.

Figure 7. Relevant morphological metrics comprise potential predictors of group impact. Silhouette tracings of species (a) bills and (b) wings demonstrate morphometric patterns. (c) Aggregate culmen and mandible lengths increase with dominance (see Fig. 5e), (d) hand wing indices predict dispersal ability (Claramunt and Wright, 2017), and (e) wing loads affect flight efficiency. Listed grey values in (c-d) are sample medians. (f) Residuals from best fit of the power model of brain volume to body mass (Krebs and Davies, 1993) compare brain sizes.

Figure 8. Small brain size and small hand wing indices drive *M*. (a-e) Raw pairwise comparisons of *M* against five covariates show broad pre-model variable relationships. (a-d) Trends are loess regressions; boxplots describe species indices from Fig. 6b. (f) Pre-trained and optimized RF models indicate brain size and hand wing index are the primary model drivers (R^2 = 0.96), bar colors correspond to (a-e) symbology. (g-j) Partial dependency plots display RF outputs, highlighting variable interaction in modeled predictions of *M* (*y*^), and the persistent importance of brain size.


a
e
d
c
b
f
*
b
c
d
e
f
g
flock abundance (no. indiv.)
0
50
100
150
200
250
300
350
0
10
20
30
40
50
60
70
80
duration (min.)
h
flock richness (no. species)
2
3
4
5
6
7
8
9
0
10
20
30
40
50
60
70
80
duration (min.)

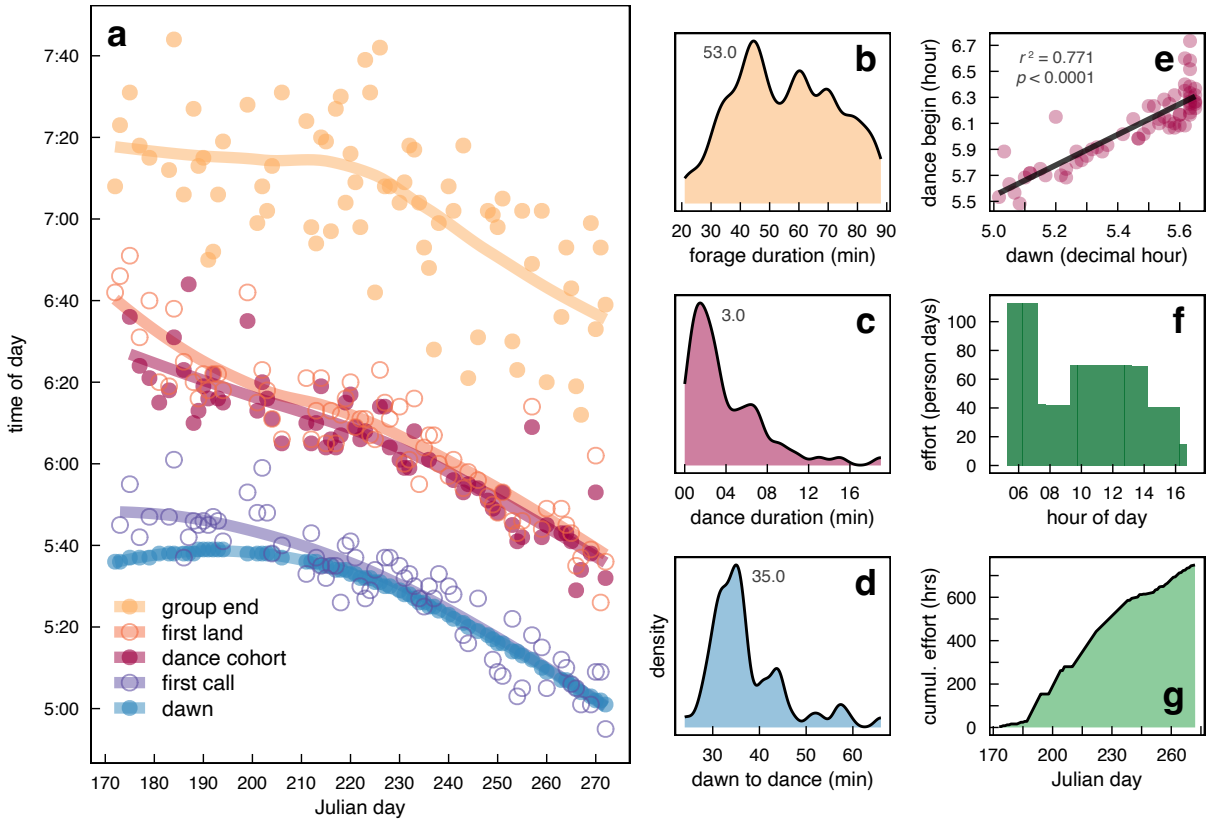
a
time of day
7:40
7:20
7:00
6:40
6:20
6:00
5:40
5:20
5:00
group end
first land
dance cohort
first call
dawn
170 180 190 200 210 220 230 240 250 260 270
Julian day
b
53.0
20 30 40 50 60 70 80 90
forage duration (min)
c
3.0
00 04 08 12 16
dance duration (min)
d
35.0
density
30 40 50 60
dawn to dance (min)
e
$r^2 = 0.771$
$p < 0.0001$
dance begin (hour)
6.7 6.5 6.3 6.1 5.9 5.7 5.5
5.0 5.2 5.4 5.6
dawn (decimal hour)
f
effort (person days)
100 80 60 40 20 0
06 08 10 12 14 16
hour of day
g
cumul. effort (hrs)
600 400 200 0
170 200 230 260
Julian day

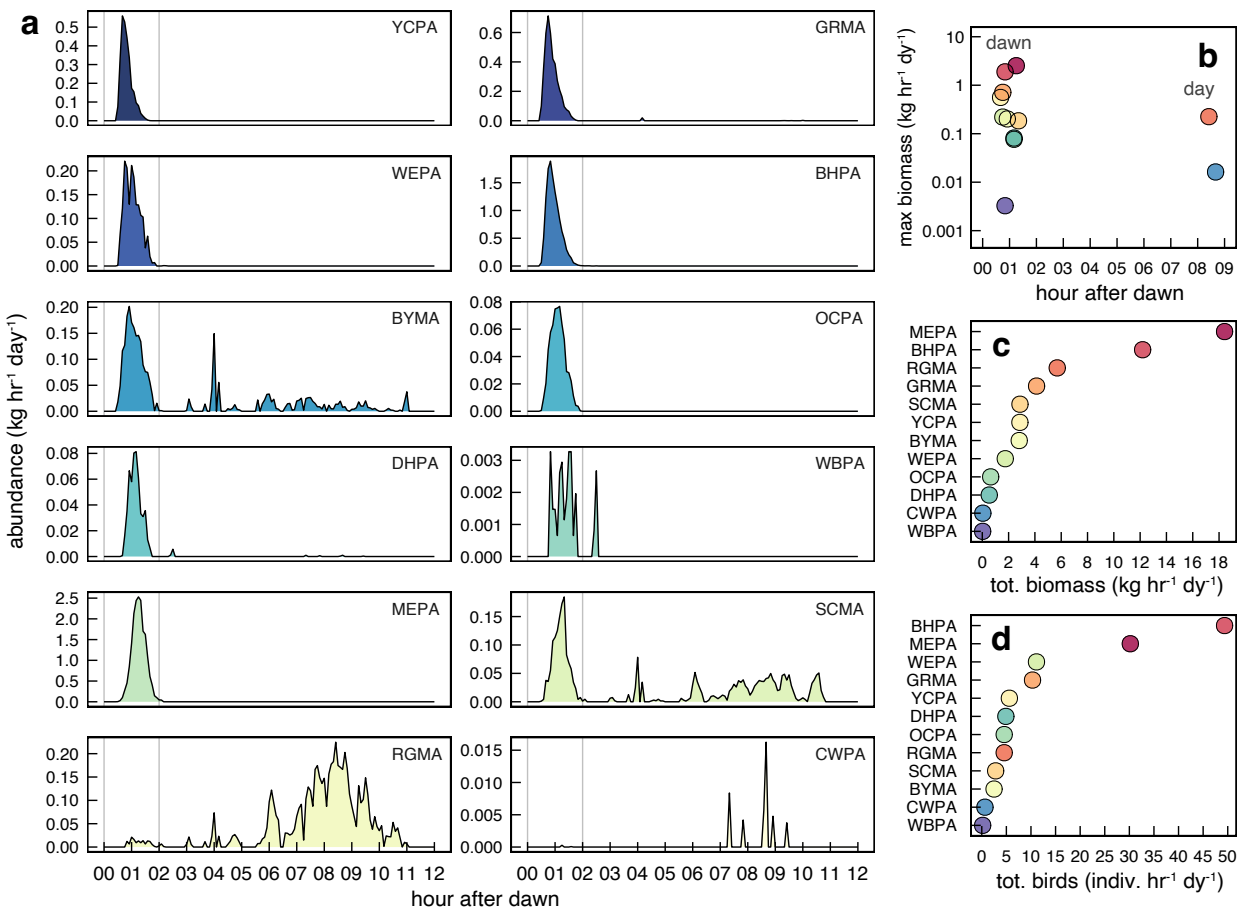
a
YCPA
GRMA
WEPA
BHPA
BYMA
OCPA
DHPA
WBPA
MEPA
SCMA
RGMA
CWPA
abundance (kg hr-1 day-1)
00 01 02 03 04 05 06 07 08 09 10 11 12
hour after dawn
b
dawn
day
max biomass (kg hr-1 dy-1)
00 01 02 03 04 05 06 07 08 09
hour after dawn
c
MEPA
BHPA
RGMA
GRMA
SCMA
YCPA
BYMA
WEPA
OCPA
DHPA
CWPA
WBPA
0 2 4 6 8 10 12 14 16 18
tot. biomass (kg hr-1 dy-1)
d
BHPA
MEPA
WEPA
GRMA
YCPA
DHPA
OCPA
RGMA
SCMA
BYMA
CWPA
WBPA
0 5 10 15 20 25 30 35 40 45 50
tot. birds (indiv. hr-1 dy-1)

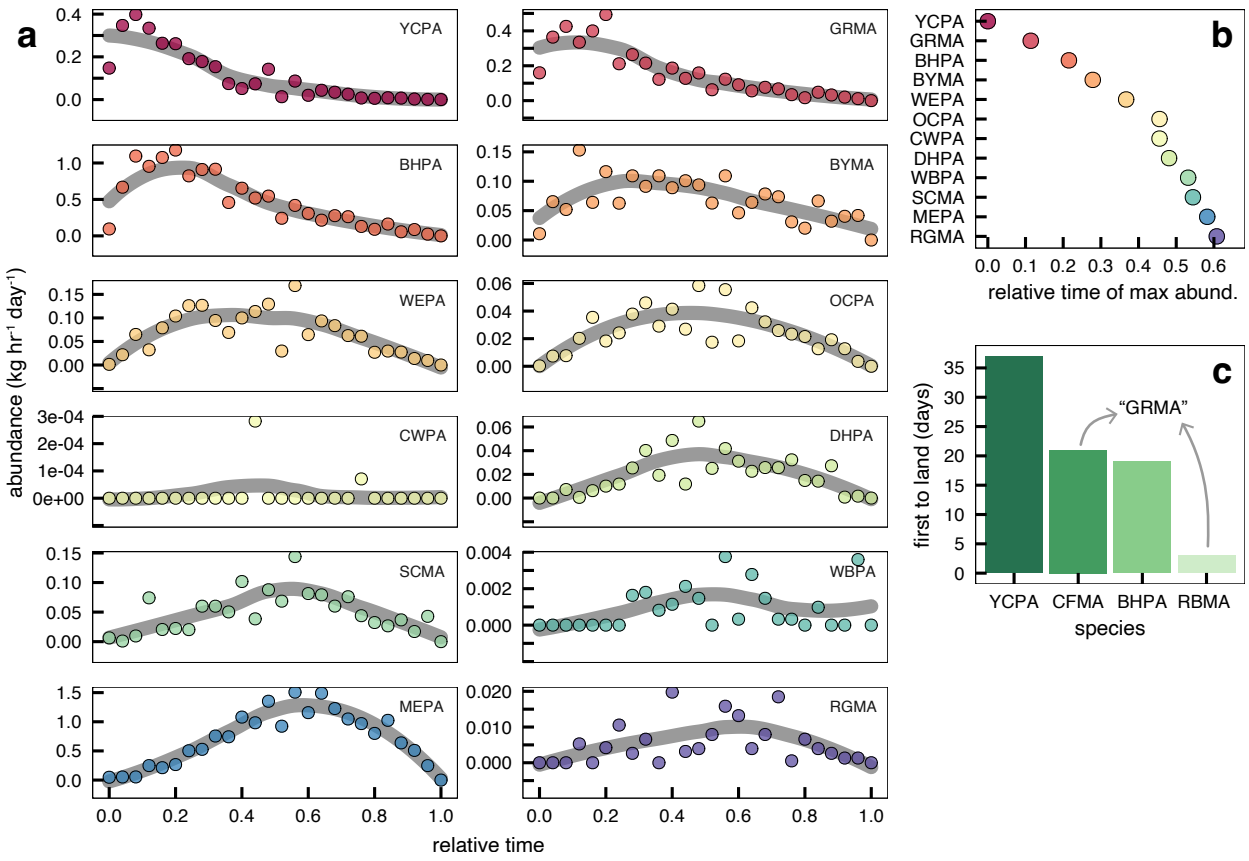
a
YCPA
GRMA
BHPA
BYMA
WEPA
OCPA
CWPA
DHPA
SCMA
WBPA
MEPA
RGMA
abundance (kg hr-1 day-1)
relative time
b
relative time of max abund.
c
first to land (days)
"GRMA"
YCPA CFMA BHPA RBMA
species

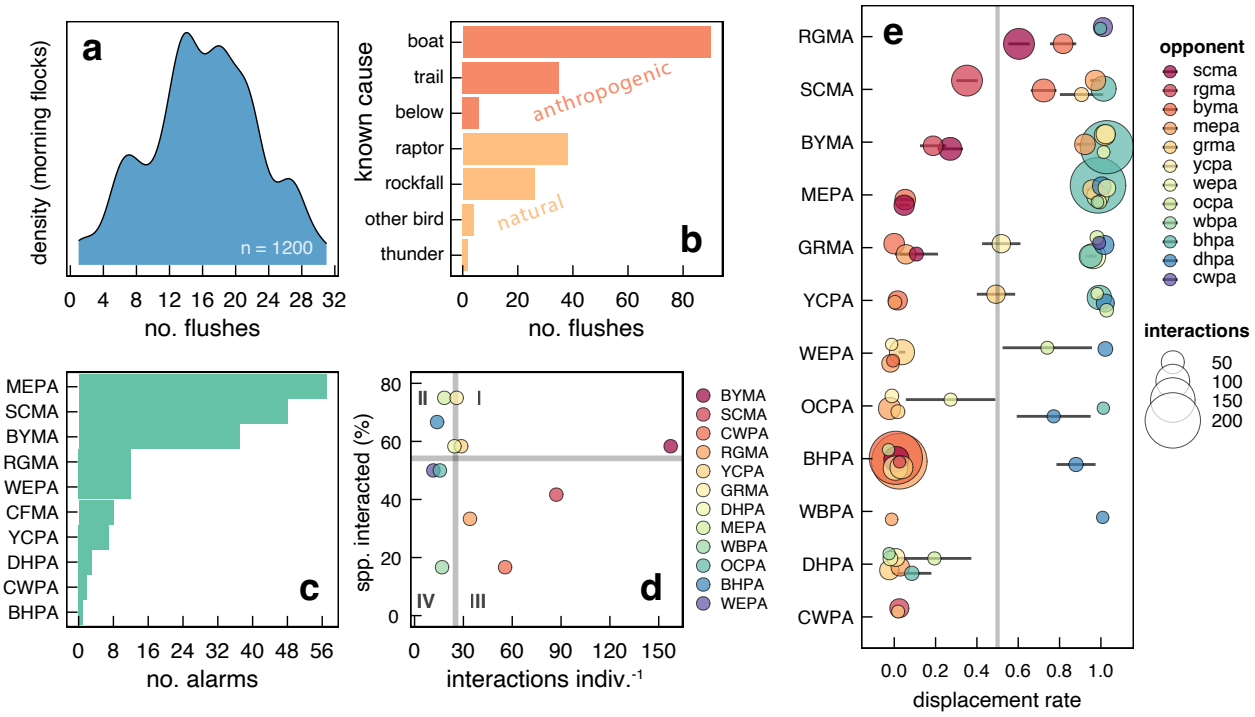
a
density (morning flocks)
n = 1200
0 4 8 12 16 20 24 28 32
no. flushes
b
known cause
boat
trail
below
raptor
rockfall
other bird
thunder
anthropogenic
natural
0 20 40 60 80
no. flushes
c
MEPA
SCMA
BYMA
RGMA
WEPA
CFMA
YCPA
DHPA
CWPA
BHPA
0 8 16 24 32 40 48 56
no. alarms
d
spp. interacted (%)
0 20 40 60 80
I
II
III
IV
0 30 60 90 120 150
interactions indiv.-1
BYMA
SCMA
CWPA
RGMA
YCPA
GRMA
DHPA
MEPA
WBPA
OCPA
BHPA
WEPA
e
RGMA
SCMA
BYMA
MEPA
GRMA
YCPA
WEPA
OCPA
BHPA
WBPA
DHPA
CWPA
0.0 0.2 0.4 0.6 0.8 1.0
displacement rate
opponent
scma
rgma
byma
mepa
grma
ycpa
wepa
ocpa
wbpa
bhpa
dhpa
cwpa
interactions
50
100
150
200

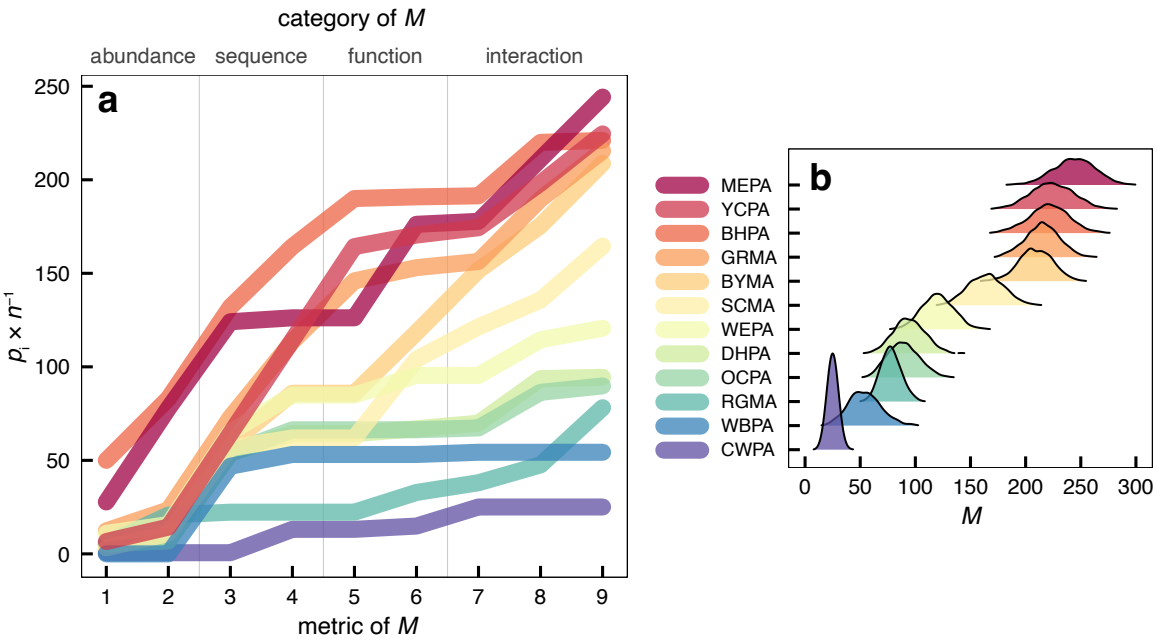
category of M
abundance
sequence
function
interaction
a
250
200
150
100
50
0
$p_i \times n^{-1}$
1
2
3
4
5
6
7
8
9
metric of M
MEPA
YCPA
BHPA
GRMA
BYMA
SCMA
WEPA
DHPA
OCPA
RGMA
WBPA
CWPA
b
0
50
100
150
200
250
300
M

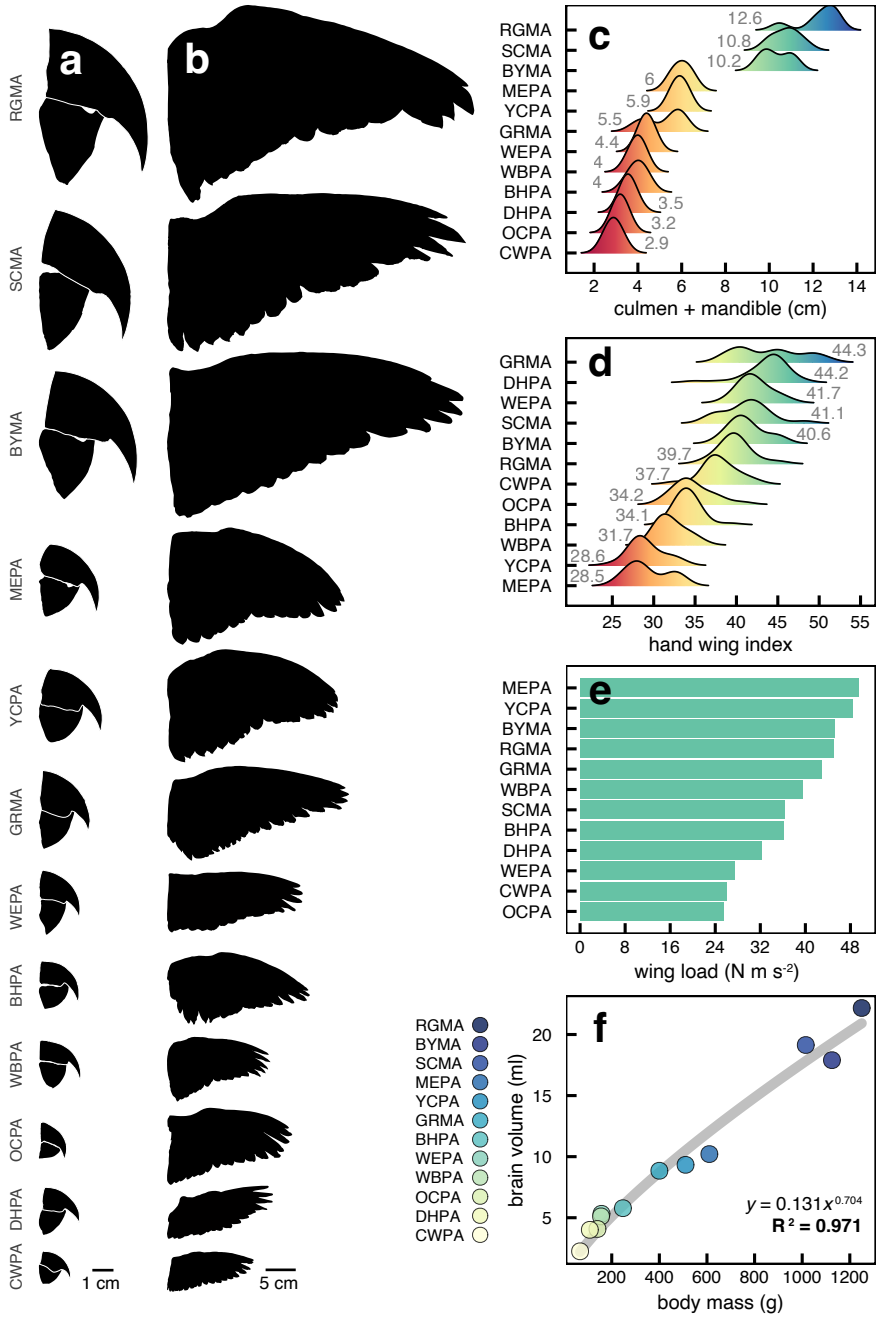
a
b
RGMA
SCMA
BYMA
MEPA
YCPA
GRMA
WEPA
BHPA
WBPA
OCPA
DHPA
CWPA
1 cm
5 cm
c
12.6
10.8
10.2
6
5.9
5.5
4.4
4
4
3.5
3.2
2.9
2 4 6 8 10 12 14
culmen + mandible (cm)
d
44.3
44.2
41.7
41.1
40.6
39.7
37.7
34.2
34.1
31.7
28.6
28.5
25 30 35 40 45 50 55
hand wing index
e
0 8 16 24 32 40 48
wing load (N m s-2)
f
brain volume (ml)
5 10 15 20
200 400 600 800 1000 1200
body mass (g)
y = 0.131x0.704
R2 = 0.971

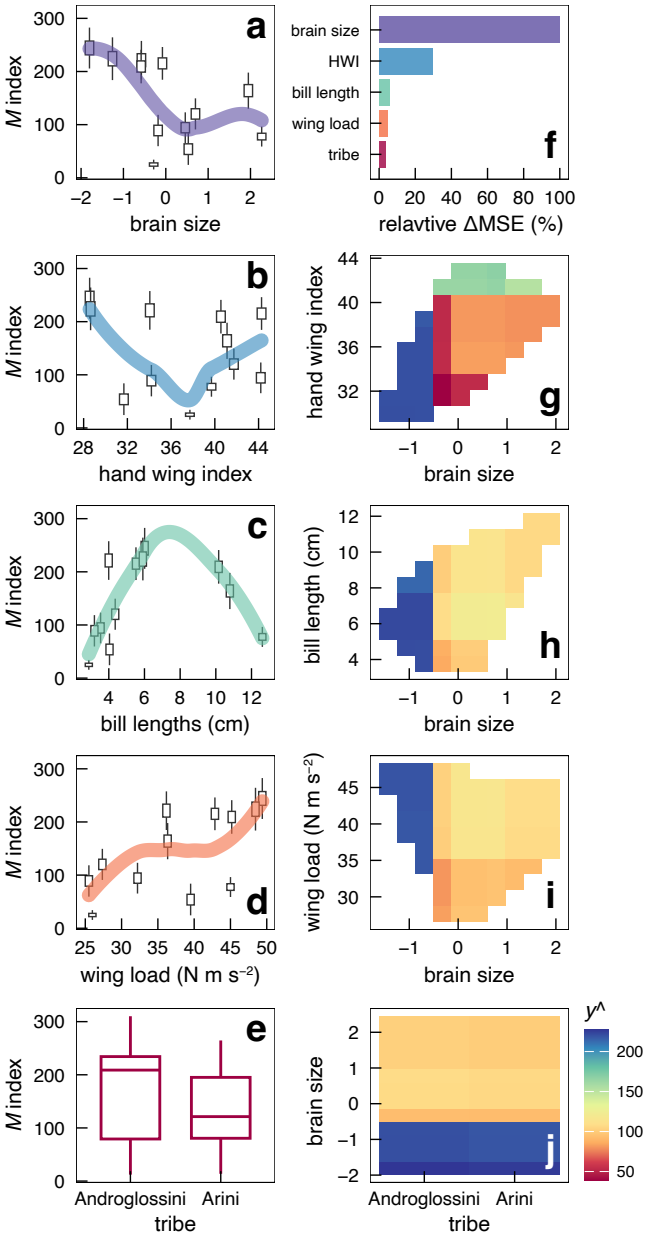
a
M index
brain size
b
hand wing index
c
bill lengths (cm)
d
wing load (N m s⁻²)
e
Androglossini
Arini
tribe
f
brain size
HWI
bill length
wing load
tribe
relavtive ΔMSE (%)
g
hand wing index
brain size
h
bill length (cm)
brain size
i
wing load (N m s⁻²)
brain size
j
brain size
Androglossini
Arini
tribe
ŷ